Accepted Manuscript - Applied Physics Letters 119, 101106 (2021). doi:10.1063/5.0060830

Electrically-injected whispering-gallery mode InGaN/GaN microdisks

K. H. Li, Y. F. Cheung, W. Y. Fu, and H. W. Choi[a)]
Department of Electrical and Electronic Engineering, the University of Hong Kong, Pokfulam Road, Hong Kong

(Dated: 9 September 2021)

The combination of high-quality factors and small mode volumes in whispering-gallery-mode (WGM) resonators promotes significantly enhanced light-matter interactions, making them excellent cavities for achieving compact semiconductor lasers with low threshold and narrow linewidth. However, success in developing GaN-based WGM lasers has been extremely limited due to the complicated design and fabrication of both high-finesse optical cavities and effective efficient injection schemes. Here, we report on WGM emission from vertical-injection blue-light emitting InGaN/GaN thin-film microdisks achieved by wafer bonding and laser lift-off removal of the sapphire substrate. The observed WGMs, identified as a combination of first order and higher order modes with the aid of finite-difference time-domain simulations, have Q-factors as high as 3700. This work presents a viable approach towards the practical implementation of compact InGaN/GaN microdisk lasers through a simple and scalable process.

The quest for high performance lasers with low threshold and high finesse has driven the rapid devlopment of low-dimensional semiconductor micro- and nano-cavities of various configurations in the last two decades[1,2]. Among various possible configurations and materials, whispering-gallery-mode (WGM) optical resonators in the form of microdisk geometries fabricated using wide bandgap GaN and its alloys are considered to be excellent candidates for achieving lasers of low threshold and high-quality factors, owing to their wide wavelength coverage, high optical gain, minuscule dimensions, as well as simple architectures[3–5]. While GaN epilayers are most commonly grown on sapphire substrates, microdisks fabricated on such wafers suffer from inefficient optical confinement due to the small refractive index contrast between the semiconductor cavity and its substrate[6]. Various pre- and post-processing strategies[4,5,7], such as the formation of undercut structures by partially removing the underlying substrate or sacrificial layers embedded within the epitaxial structure, have been developed to optically isolate the microdisk cavity; however such undercut structures are mostly incompatible with electrical injection schemes due to the electrically insulating substrate. Recently, electrically-injected GaN microdisks and microrings on silicon, GaN and copper substrates have been reported[8–14]. Nevertheless, progress in this field has been severely limited due to the stringent design and fabrication requirements imposed by both optical confinement and electrical injection, limiting their practical applications. In this work, by forming InGaN/GaN thin-film microdisks on an electrically-conducting and optically-reflective metal film, WGM emission in electrically-injected GaN microdisks at room temperature (RT) under continuous-wave (CW) operation is demonstrated. Such microdisk WGM resonators have good prospects of becoming a core building blocks of next-generation compact-size, low-power, and high-speed photonic circuits[15,16].

The proposed thin-film microdisk structure, illustrated in the schematic diagram of Fig. 1(a), is designed to facilitate electrical injection and optical confinement simultaneously. The top p-type GaN surface of the wafer is bonded to a metal-coated Si wafer via eutectic bonding, followed by laser lift-off (LLO) for removal of the sapphire substrate.[17] The Ni/Ag/Ni/Au interfacial bonding layer, which provides reflectance of 71-77% across the blue spectral range of 440-475 nm as shown in Fig. 1(b), serves not just as a reflector for the bottom surface of the microdisk but also as ohmic contact for the p-electrode. Incidentally, the high thermal conductivity of the metal layer also facilitate heat dissipation from the microdisk enabling high-current-density operation.

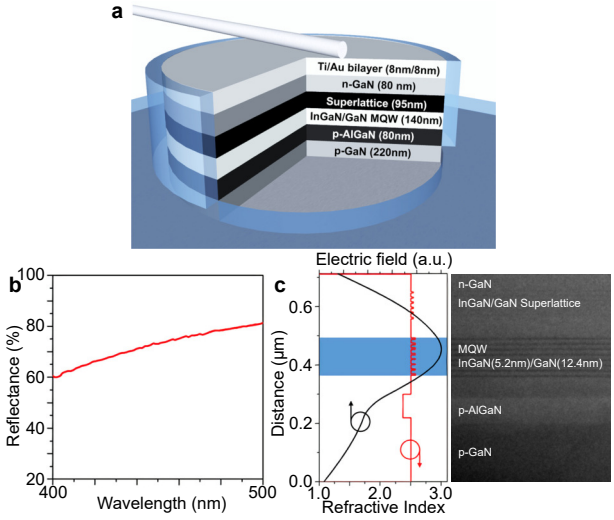

FIG. 1. (a) Schematic diagram of the 5.6-μm InGaN/GaN microdisk. (b) Measured reflectance of the bottom Ni/Ag/Ni/Au layer. (c) Calculated profile of the electric field distribution (left) and a cross-sectional TEM image of the epitaxial structure (right).

Due to the absence of an optical cladding layer, the thick as-grown epitaxial structure is not conducive to optical confinement along the vertical direction, which can be improved by reducing the cavity thickness. As the QW active region is located near the bottom of the thick epi-structure, the transferred GaN film can be thinned down to sub-micron thickness by dry-etching away the excessive layers. The electric field amplitude distribution in such a thin-film structure as shown

[a)]Electronic mail: hwchoi@hku.hk

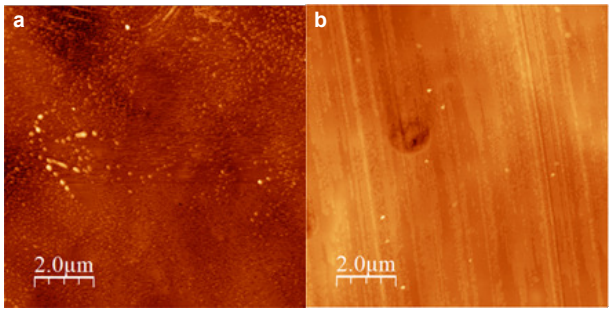

FIG. 2. AFM images measured from (a) p-GaN and (b) n-GaN surfaces of the transferred film after LLO followed by ICP deep etching.

in Fig. 1(c) is calculated by taking into account the bottom metallic reflector, showing an asymmetrical profile. Although the bottom metal layer is a lossy medium and absorbs a finite amount of light to affect the mode profile, the reduced epi-thickness allows the field maximum coincides well with the InGaN/GaN active region, giving estimated confinement factor and modal gain of 0.31 and 0.025 respectively.

The surface morphology of the substrate-removed GaN thin film plays an instrumental role in determining the light confinement ability of the microdisk cavity. As shown by the Atomic Force Microscopy (AFM) images in Fig. 2, an optically smooth surface is retained for top n-GaN and bottom p-GaN surfaces with root-mean-square roughness of 6.0 nm ($\sim\lambda/76$) and 2.0 nm ($\sim\lambda/230$) respectively.

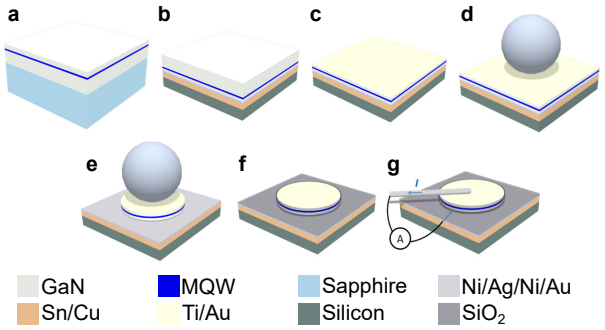

FIG. 3. Schematic diagrams illustrating the fabrication process. (a) As-grown. (b) Wafer bonding to Si substrate followed by sapphire detachment by LLO. (c) n-GaN layer thinned down by ICP etching. (d) Spin coating of microspheres (e) Pattern transfer by ICP etching. (f) SiO_2 coating before lift-off of microspheres. (g) Wire bonding using Ag nanowire.

The planar microdisk resonator is a simple yet efficient geometry that supports WGMs in which optical waves are guided along the disk circumference by continuous internal reflection[1]. As such, accurate wavelength-scale patterning techniques are required for precise pattern definition. At the same time, the need for etching through the hard GaN film with high etch selectivity and anisotropy calls for a hard mask that can withstand the etch with minimal mask erosion[18]. Instead of conventional lithographic techniques involving soft photoresist, the approach of microsphere lithography (MSL) is adopted. MSL is a cost-effective and high-throughput patterning technique based on the self-assembly of microspheres, which is ideal for forming individual, clusters or even hexagonal-closed-packed arrays of circular micro- and nanostructures. In particular, the use of silica microspheres for this purpose has been demonstrated to provide high etch selectivity over GaN to form microdisks of excellent circularity with smooth and vertical sidewalls[19].

The remaining challenge lies with establishing an electrical connection to the small microdisks, whose dimensions are much smaller than typically bonding pads. Although methods of gap filling, such as the use of spin-on-glass (SOG)[20], can be applied to planarize large-area non-planar surfaces, the reduction in refractive index contrast at the microdisk boundaries will significantly weaken optical confinement within the microdisk. Formation of sub-micron scale air-bridge contacts[11,13] would be an alternative solution but relies heavily on an electron-beam lithographic step for alignment, making it unsuitable for large-area integration. The robustness of the air-bridge is also a subject of concern. A lithographic-free contact technology is adopted in this work that makes use of low-resistance and high-optical-transmittance Ag nanowires as bonding wires. By fusing the nanowires with the top microdisk contact by thermal annealing, electrical injection to the microdisks can be established in an uncomplicated way.

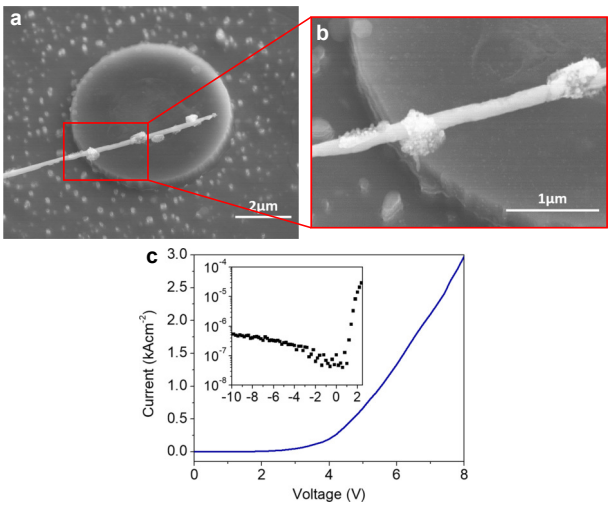

FIG. 4. (a) SEM image of the resultant 5.6-μm InGaN/GaN microdisk. (b) Close-up view showing the bonding of Ag nanowire. (c) I-V characteristics of the microdisk measured at room temperature; the inset shows the I-V curve on a semi-log scale.

The epitaxial structure used in this work is grown on 2-inch *c*-plane sapphire substrates by metal-organic chemical vapor deposition (MOCVD), consisting of undoped GaN, n-doped GaN, 8 pairs of $In_{0.11}Ga_{0.89}N$/GaN quantum-wells (QWs) (5.2nm/12.4nm), and p-doped GaN layers, as illustrated in Fig. 1(c) and Fig. 3(a). The internal quantum efficiency of the MQWs is determined to be > 70% (see Supplementary Section 1). Ni/Ag/Ni/Au (8nm/100nm/25nm/50nm) multi-layers are deposited over the p-GaN surface by electron-beam (e-beam) evaporation while Ti/Au (30nm/100nm) bi-layers are

coated on bare Si wafers, followed by rapid thermal annealing (RTA). Cu-Sn intermetallic layers are then electroplated over the seed-conduction layers. By making use of Cu-Sn solid-liquid inter-diffusion bonding, the wafer is wafer-bonded onto the Si substrate using an EVG 501 bonder. The collimated beam from a frequency-quadrupled 266-nm Nd:YAG laser is uniformly irradiated onto the polished sapphire surface, and the sapphire substrate is readily removed due to decomposition of interfacial GaN into Ga droplets and gaseous N_2, as depicted in Fig. 3(b). After removal of the substrate, the ∼7-μm GaN film is thinned down to ∼700 nm by BCl_3-based inductively-coupled plasma (ICP) etching. A bi-layer of Ti/Au (5nm/5nm) is e-beam deposited over the sample, as shown in Fig. 3(c). Colloidal suspensions of silica microspheres are dispensed onto the thinned-down surface using a micropipette which are then sparsely dispersed by spin-coating, as illustrated in Fig. 3(d). The spheres serve as a lithographic hard mask so that the microdisk pattern is transferred to the GaN thin-film during ICP etching using Cl_2/He gas mixtures. The exposed GaN sidewall surface is oxidized using an O_2 plasma in a reactive ion etching (RIE) chamber for 2 min. The sample is then dipped in an HCl: H_2O (1:10) solution for 1 min to remove the oxidized layer. After three cycles of "digital etching"[21], an SiO_2 layer is electron-beam deposited over the entire surface. Following lift-off of the spheres by sonication in deionized water, the top n-GaN surface of the microdisk is exposed while the sidewall remains covered by the SiO_2 layer, as shown in Fig. 3(f). Ag nanowires serving as metal bonding wires are sparsely-dispersed over the sample by spin-coating, followed by a mild thermal annealing process (see Supplementary Sections 2 and 3) for fusing one end of the nanowire onto the n-contact of the microdisk for robust bonding. The other end of the nanowire is electrically contacted with a microprobe tip. As depicted in Fig. 3(g), the microdisk can be electrically injected by by applying a bias voltage between the Ag nanowire and the planar p-contact layer.

A scanning electron microscopy (SEM) image of the fabricated device is shown in Fig. 4 (a), from which a 5.6-μm microdisk attached on the metal film of a Si substrate and bonded with an Ag nanowire is seen. The image in Fig. 4(b) shows the robust fused connection between the microdisk top contact and the Ag nanowire. The current-voltage (I-V) characteristics of the vertical-injection device are measured under forward and reverse biased conditions with a Keithley Instrument 2401 Source Measure Unit. From the plot of Fig. 4(c), the turn-on voltage is found to be 4.2 V and the series resistance determined through the inverse slope of the linear region of the curve is 1.3 mΩ cm^2. Moreover, the treatments on the etched sidewall, including removal of plasma-induced damage by digital etching and sidewall preservation with a thin oxide layer, are effectively suppressing non-radiative recombination at the sidewalls, resulting in very low reverse leakage currents as shown in the inset in Fig. 4(c).

Emission characteristics of the GaN microdisks are investigated under CW current injection at RT. Fig. 5(a) shows the measured electroluminescence (EL) spectra of the microdisk device. The EL signals from microdisks are collected with an optical fiber in the near-horizontal direction, coupled to an

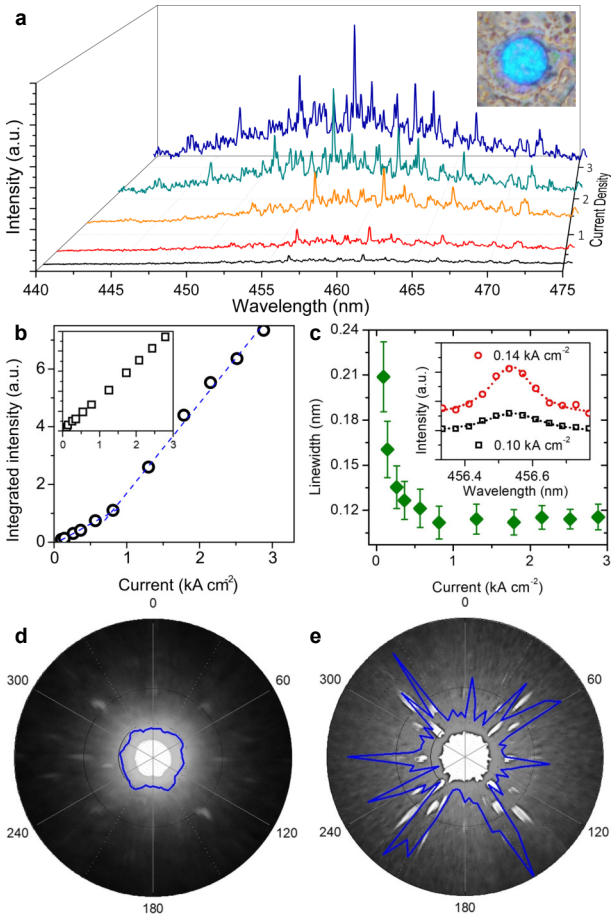

FIG. 5. (a) EL spectra of 5.6-μm InGaN/GaN microdisk measured under different current densities. (b) Integrated intensity and (c) spectral linewidth of the peak at 456.5 nm as a function of injection-current density and the inset shows the fitted Lorentzian lineshapes for the two lowest current densities. In-plane far-field intensity profiles in polar coordinate of the microdisk excited (d), below ($0.66I_{th}$) and (e), above the threshold ($3.8I_{th}$), superimposed on top of which are the corresponding top-view micrographs captured through a 50× objective with a numerical aperture of 0.8.

Acton SP2500A spectrometer comprising a 500 mm spectrograph and a Princeton Instrument PIXIS open-electrode CCD, offering optical resolutions of 0.04 nm. It is observed that sharp spectral peaks are superimposed on a broad emission background and the peak centered at 456.5 nm is dominant over the others. Fig. 5(b) plots the integrated intensity of the spectral peak at 456.5 nm as a function of current density with observation of a kink at around 0.85 kA cm^{-2} that is not present in the corresponding plot for the broad background emission plotted in the inset of Fig. 5(b) which exhibits linear L-I characteristic. The plot in Fig. 5(c) shows spectral linewidth narrowing approaching the threshold, with a minimum value of 0.11 nm around the threshold. The nonlinear increase of the emission intensity and spectral narrowing near the threshold seems to suggest achievement of lasing, although the kink in the L-I curve at the threshold shown in Fig. 5(b) may not sharp enough to be conclusive. The quality

factor (Q) is evaluated as ~3700 based on $Q = \lambda/\Delta\lambda$ under sub-threshold conditions of $0.66I_{\text{th}}$.

Fig. 5(d), (e) shows measured angular radiation distribution of the microdisk for excitation conditions below and above the threshold respectively superimposed over the corresponding top-view microscopic images of the microdisks. The far-field radiation plots in the near-planar direction are measured by rotating the microdisk in steps of 5 degrees. The collection angle of the optical fiber is maintained at 80 degrees from the normal while the separation between the microdisk and the optical fiber is fixed at 4 cm. Below the threshold, emission is mostly spontaneous, revealing a homogeneous intensity distribution along the microdisk circumference. Above the threshold, the radiation is partially scattered out of the cavities through imperfections at the boundary, resulting in a high degrees of emission directionality at various discrete angles.

The resonant wavelength and free spectral range (FSR) of the microdisk cavity are analyzed through 2D simulations via the finite-difference time-domain (FDTD) method. The computational mesh size is fixed at 5 nm, with the time step set to 0.0035 fs satisfying the Courant stability condition. Only TE modes are considered, as the light emitted from InGaN/GaN QWs is predominately TE polarized (see Supplementary Section 4). The simulated WGM resonances within the microdisk cavity are displayed in Fig. 6, together with the mode numbers (n, m) being labeled for these dominant optical modes, where n and m represent the mode numbers in the radial and azimuthal directions, respectively. The dominant spectral peaks are found to belong to the first order WGM family ($n = 1$) while other less intense peaks correspond to higher radial order WGMs (see Supplementary Sections 5), attributed to an increase in radiation loss with reducing bend radius.

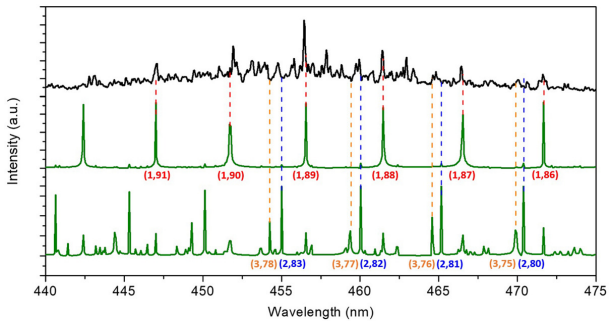

FIG. 6. EL spectra from the 5.6-μm microdisk at the excitation condition of ~$3.8I_{\text{th}}$. The green plots show the simulated optical resonances within the microdisk cavity as predicted by FDTD simulations. The spectra have been offset vertically for clarity.

The measured high Q-factor of ~3700 under electrical injection implies low optical losses in the microdisk cavity, which is related to three major factors, namely radiation loss, absorption loss, and scattering loss. The radiation loss has a negligible influence on Q due to the large refractive index contrast at the GaN/air interface. The absorption loss approaches zero within the emission band when the excitation threshold has been reached. The scattering loss is governed by the surface smoothness of the WGM resonator. For the microdisk cavity which is formed by top-down etching, the surface roughness of the etched sidewall facet is often a major factor degrading WGM confinement due to scattering losses. Geometrical irregularities and sidewall roughness resulting from mask erosion[22] are also transferred onto the GaN microdisk, further degrading the confinement ability of the cavity. Therefore, apart from ensuring high optical smoothness at the top and bottom surfaces, the SiO_2 microsphere has positively contributed to the well-defined geometry of the microdisk.

The fabrication process benefits from a high degree of scalability, both in terms of the number and density of microdisks on a chip, as well as the dimensions of the individual microdisks. Arraying of microdisks can readily be achieved by precisely controlling the density of the dispersed microspheres on the sample, while the dimensions are determined by the diameters of the microspheres used. As the number of modes is proportional to the diameter of the microdisk, single mode emission may be attained through the use of microspheres of sub-micron diameters.

In conclusion, we have demonstrated WGM emission in a GaN microdisk under CW-RT electrical injection. The vertical-injection microdisks on a metallic reflector with smooth sidewalls and good circularity are fabricated through preparation of a GaN-on-metal platform by LLO and subsequent pattern transfer by MSL. A nanoscale wire-bonding process is developed to achieve effective surface passivation and bonding of metal nanowires onto the microdisks, which simplifies the current injection scheme and allows for more design flexibility and lower packaging costs. The WGM characteristics measured from the fabricated microdisks are in good agreement with theoretical predictions and simulation results. The realization of compact blue-emitting microdisk resonators adopting a controllable and scalable approach is attractive for applications such as micro-lasers, sensing, quantum optics, high-speed communications, information processing, and optical interconnects.

SUPPLEMENTARY MATERIAL

See the supplementary material for power-dependent IQE graph, SEM images on the self-assembled microspheres and Ag nanowires, a discussion on the effect of thermal annealing on Ag nanowires, polarization properties on microdisk, and further analysis on the WGMs.

ACKNOWLEDGEMENTS

This work was supported by the ANR/RGC Joint Research Scheme sponsored by the Research Grant Council of Hong Kong SAR and French National Research Agency (Project A_HKU703/17).

DATA AVAILABILITY

The data that supports the findings of this study are available within the article and its supplementary information files and from the corresponding author upon reasonable request.

REFERENCES

[1] K. J. Vahala, "Optical microcavities," Nature **424**, 839–846 (2003).

[2] H. Matsubara, S. Yoshimoto, H. Saito, J. L. Yue, Y. Tanaka, and S. Noda, "Gan photonic-crystal surface-emitting laser at blue-violet wavelengths," Science **319**, 445–447 (2008).

[3] S. L. Mccall, A. F. J. Levi, R. E. Slusher, S. J. Pearton, and R. A. Logan, "Whispering-gallery mode microdisk lasers," Applied Physics Letters **60**, 289–291 (1992).

[4] H. W. Choi, K. N. Hui, P. T. Lai, P. Chen, X. H. Zhang, S. Tripathy, J. H. Teng, and S. J. Chua, "Lasing in gan microdisks pivoted on si," Applied Physics Letters **89** (2006), 10.1063/1.2392673.

[5] A. C. Tamboli, E. D. Haberer, R. Sharma, K. H. Lee, S. Nakamura, and E. L. Hu, "Room-temperature continuous-wave lasing in gan/ingan microdisks," Nature Photonics **1**, 61–64 (2007).

[6] M. Kneissl, M. Teepe, N. Miyashita, N. M. Johnson, G. D. Chern, and R. K. Chang, "Current-injection spiral-shaped microcavity disk laser diodes with unidirectional emission," Applied Physics Letters **84**, 2485–2487 (2004).

[7] E. D. Haberer, R. Sharma, C. Meier, A. R. Stonas, S. Nakamura, S. P. DenBaars, and E. L. Hu, "Free-standing, optically pumped, gan/ingan microdisk lasers fabricated by photoelectrochemical etching," Applied Physics Letters **85**, 5179–5181 (2004).

[8] M. X. Feng, J. L. He, Q. Sun, H. W. Gao, Z. C. Li, Y. Zhou, J. P. Liu, S. M. Zhang, D. Y. Li, L. Q. Zhang, X. J. Sun, D. B. Li, H. B. Wang, M. Ikeda, R. X. Wang, and H. Yang, "Room-temperature electrically pumped ingan-based microdisk laser grown on si," Optics Express **26**, 5043–5051 (2018).

[9] J. Wang, M. X. Feng, R. Zhou, Q. Sun, J. X. Liu, X. J. Sun, X. H. Zheng, M. Ikeda, X. Sheng, and H. Yang, "Continuous-wave electrically injected gan-on-si microdisk laser diodes," Optics Express **28**, 12201–12208 (2020).

[10] Y. Mei, M. C. Xie, H. Xu, H. Long, L. Y. Ying, and B. P. Zhang, "Electrically injected gan-based microdisk towards an efficient whispering gallery mode laser," Optics Express **29**, 5598–5606 (2021).

[11] J. Wang, M. X. Feng, R. Zhou, Q. Sun, J. X. Liu, Y. N. Huang, Y. Zhou, H. W. Gao, X. H. Zheng, M. Ikeda, and H. Yang, "Gan-based ultraviolet microdisk laser diode grown on si," Photonics Research **7**, B32–B35 (2019).

[12] J. Wang, M. X. Feng, R. Zhou, Q. SUn, J. X. Liu, X. J. Sun, X. H. Zheng, X. Sheng, and H. Yang, "Thermal characterization of electrically injected gan-based microdisk lasers on si," Applied Physics Express **13** (2020), 10.35848/1882-0786/ab95f0.

[13] F. Tabataba-Vakili, S. Rennesson, B. Damilano, E. Frayssinet, J. Y. Duboz, F. Semond, I. Roland, B. Paulillo, R. Colombelli, M. El Kurdi, X. Checoury, S. Sauvage, L. Doyennette, C. Brimont, T. Guillet, B. Gayral, and P. Boucaud, "Iii-nitride on silicon electrically injected microrings for nanophotonic circuits," Optics Express **27**, 11800–11808 (2019).

[14] H. Zi, W. Y. Fu, F. Tabataba-Vakili, H. Kim-Chauveau, E. Frayssinet, P. De Mierry, B. Damilano, J. Y. Duboz, P. Boucaud, F. Semond, and H. W. Choi, "Whispering-gallery mode ingan microdisks on gan substrates," Optics Express **29**, 21280–21289 (2021).

[15] F. Tabataba-Vakili, L. Doyennette, C. Brimont, T. Guillet, S. Rennesson, E. Frayssinet, B. Damilano, J. Y. Duboz, F. Semond, I. Roland, M. El Kurdi, X. Checoury, S. Sauvage, B. Gayral, and P. Boucaud, "Blue microlasers integrated on a photonic platform on silicon," Acs Photonics **5**, 3643–3648 (2018).

[16] C. H. To, W. Y. Fu, K. H. Li, Y. F. Cheung, and H. W. Choi, "Gan microdisk with direct coupled waveguide for unidirectional whispering-gallery mode emission," Optics Letters **45**, 791–794 (2020).

[17] X. Zhang, Y. F. Cheung, Y. Zhang, and H. W. Choi, "Whispering-gallery mode lasing from optically free-standing ingan microdisks," Optics Letters **39**, 5614–5617 (2014).

[18] S. J. Pearton, J. C. Zolper, R. J. Shul, and F. Ren, "Gan: Processing, defects, and devices," Journal of Applied Physics **86**, 1–78 (1999).

[19] W. N. Ng, C. H. Leung, P. T. Lai, and H. W. Choi, "Photonic crystal light-emitting diodes fabricated by microsphere lithography," Nanotechnology **19**, 255302 (2008).

[20] H. M. Kim, Y. H. Cho, H. Lee, S. I. Kim, S. R. Ryu, D. Y. Kim, T. W. Kang, and K. S. Chung, "High-brightness light emitting diodes using dislocation-free indium gallium nitride/gallium nitride multiquantum-well nanorod arrays," Nano Letters **4**, 1059–1062 (2004).

[21] D. Buttari, S. Heikman, S. Keller, and U. K. Mishra, "Digital etching for highly reproducible low damage gate recessing on algan/gan hemts," in *Proceedings. IEEE Lester Eastman Conference on High Performance Devices*, pp. 461–469.

[22] S. J. Pearton, R. J. Shul, and F. Ren, "A review of dry etching of gan and related materials," Mrs Internet Journal of Nitride Semiconductor Research **5**, 1–38 (2000).